Hard X-ray Photon-In Photon-Out Spectroscopy

Pieter Glatzel [a]; Frank M. F. de Groot [b]; Uwe Bergmann [c]

[a] European Synchrotron Radiation Facility, Grenoble, France [b] Inorganic Chemistry and Catalysis, Debye Institute for Nanomaterials Science, Utrecht University, Utrecht, The Netherlands [c] Stanford Synchrotron Radiation Laboratory, Stanford, CA, USA

PLEASE SCROLL DOWN FOR ARTICLE

Hard X-ray Photon-In Photon-Out Spectroscopy

Pieter Glatzel[1], Frank M. F. de Groot[2], Uwe Bergmann[3]

[1]*European Synchrotron Radiation Facility, Grenoble, France*

[2]*Inorganic Chemistry and Catalysis, Debye Institute for Nanomaterials Science, Utrecht University, Utrecht, The Netherlands*

[3]*Stanford Synchrotron Radiation Laboratory, Stanford, CA, USA*

X-ray absorption spectroscopy (XAS) has become an indispensable tool in catalysis research. The instrumentation at synchrotron radiation sources as well as analysis and calculation of XAS has reached such a high level that this technique is now attractive to a very large user community. Standard XAS, however, cannot answer all questions and complementary techniques that address the electronic structure in more detail and help to investigate low Z elements as ligand or absorber add to the repertoire of hard X-ray techniques. We discuss in this contribution how energy analysis of the scattered photons [1] in addition to control of the incident photon energy (cf. Figure 1) extends the range of applications of XAS and addresses some problems that XAS cannot solve [2].

The instrumental energy bandwidth in XAS is on the order of the core hole lifetime broadening, which is around 1 eV for 3d transition metal K edges. Hard X-ray monochromators are typically based on perfect-crystal Bragg optics for the incident photons and the same principle can be used to analyze the scattered photons. Various geometries using spherical, cylindrical and flat crystals with point-to-point or dispersive geometries have been realized at synchrotron radiation beamlines [3]. We show in Figure 2 a point-to-point Rowland geometry with five spherically bent crystals.

A number of spectroscopic techniques become available using such an experimental setup [4]. They can be grouped into:

- High-Energy Resolution Fluorescence Detected (HERFD) XAS;
- X-ray Raman Spectroscopy (XRS);
- Non-Resonant X-ray Emission Spectroscopy (XES);
- Resonant X-ray Emission Spectroscopy (RXES) and resonant inelastic X-ray scattering (RIXS).

The first two techniques complement and improve the current standard XAS experiments while the last two open up possibilities for detailed studies of the electronic structure using a photon-in photon-out technique. The hard X-ray probe makes all techniques suitable for *in-situ* (*operando*) studies and experiments under extreme conditions (*e.g.* high pressure).

High-energy resolution fluorescence detected (HERFD) XAS

Fluorescence detected XAS takes advantage of a secondary process— the radiative decay of photoexcited states—which is to a very good approximation proportional to the absorption coefficient. An energy dispersive solid state detector provides an energy bandwidth of about 200–300 eV at the Fe Kα line. The captured solid angle depends on the number of elements used and the distance from the sample and can be as high as 0.4 sr. Non-linearity at high count-rates often limits the use of solid state detectors at high flux synchrotron radiation beamlines. An X-ray spectrometer allows one to choose the X-ray detector freely because the energy is selected by means of Bragg optics [5]. This ensures a dramatic reduction of unwanted background radiation (only photons of interest reach the detector) and increase of usable dynamic range. Thus, measurements of up to 10^7 counts/sec with basically no background in the desired fluorescence line become feasible using, e.g., an Avalanche Photo Diode (APD) as X-ray detector. The XES solid angle is limited by geometrical constraints of the emission spectrometer. Current multi-crystal spectrometers reach 0.04–0.1 sr. Also, the reflectivity of the analyzer crystals is currently only at 10%. Developments towards smaller bending radii of the analyzer crystals, and thus solid angles up to 0.3 sr, as well as higher efficiency, will make XES for many experiments a viable competitor to solid state detectors at orders of magnitude better energy resolution. The additional freedom to use a very fast detector is particularly interesting for time-resolved studies.
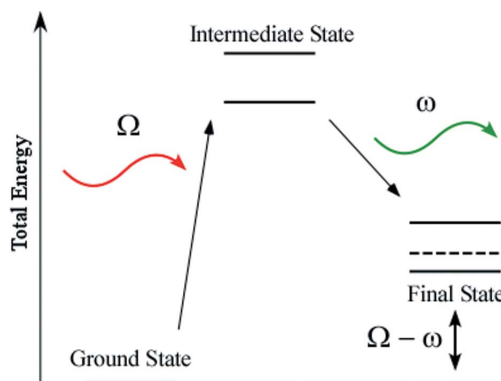

Figure 1: Energy scheme for photon-in (Ω) and photon-out (ω) spectroscopy. The intermediate states give rise to an absorption spectrum. The total energy of the final states is given by the energy transfer Ω-ω.

HERFD XAS offers the best possible signal-to-background ratio because the energy resolution is on the order of the core hole lifetime broadening. An important consequence is the suppression of diffraction peaks in XAS measurements of polycrystalline samples. The ideal separation of fluorescence lines in XES further-more allows us to record EXAFS in dilute samples beyond unwanted absorption edges [6], e.g. Mn EXAFS in the presence of Fe [7].

The spectral features in HERFD XAS can be sharper than the core hole lifetime broadening [8]. The K absorption pre-edges in 3d transition metals can thus be better separated from the main edge. This approach has been used to study the local symmetry at the metal site of Mn and Fe/ZSM5 catalysts [9]. The differences between standard and HERFD XAS have been discussed by Carra et al. [10], who pointed to the pitfalls of this technique when attempting to record a true absorption spectrum, and their ideas have been illustrated by several other authors [2, 11]. It was found that HERFD XAS on 5d transition elements can be interpreted to good accuracy as XAS spectra measured below the core hole lifetime broadening (cf. Figure 1) and the technique has been employed to study CO adsorption on Pt and to identify partially oxidized Au/Al_2O_3 as reaction intermediate [12].

X-ray Raman scattering

Inelastic scattering of hard X-rays by excitation of an inner-shell electron into an unoccupied state is often referred to as X-ray Raman Scattering (XRS) or non-resonant inelastic X-ray scattering (NIXS). This non-resonant process has an extremely small cross section ($10^{-5} – 10^{-4}$ that of XAS) but is very powerful for two reasons: a) one can obtain soft X-ray XAS information with hard X-rays; and b) one can study dipole forbidden transitions, i.e. final states not accessible with con-ventional XAS. The advantages of using a hard X-ray probe for light elements and/or low energy (~50–500 eV) excitations can be exploited in different ways. First, one can get true bulk information (see e.g. the work on hydrocarbons including asphaltenes [13], Fig. 3). Second, one can take advantage of the high spectral stability and reproducibility of perfect crystal Bragg optics in the multi keV range to obtain high quality spectra that make possible the observation of very small spectral changes and even EXAFS [14]. Such studies have previously not been possible with soft X-rays at the O K-edge. Third, gases, windows, and gaskets of *in situ* and high pressure cells can be penetrated in studies of materials under chemically relevant *in situ* or extreme conditions [15].

In addition to these advantages with regards to the sample condi-tion and environment, XRS carried out at large momentum transfers q
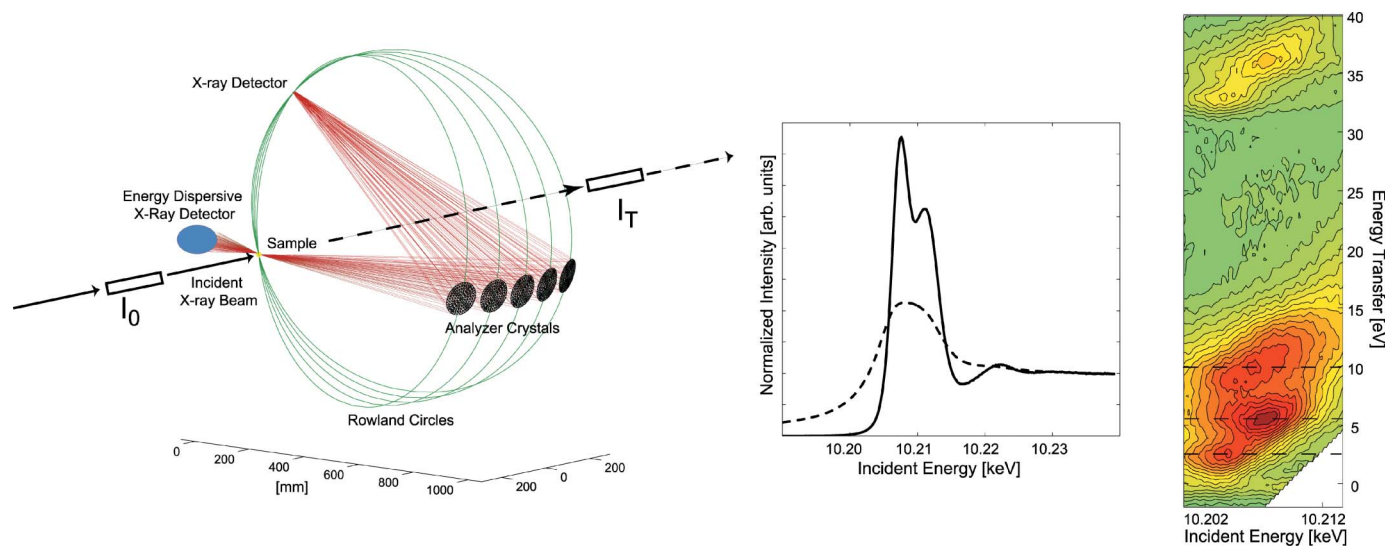
Figure 2: (left) Schematic experimental setup for XAS in transmission, medium and high energy resolution fluorescence detection mode; (center) standard (dashed line) and high resolution XAS of 2 at % W in TiO$_2$; (right) RIXS plane of W in WO$_2$; the dashed lines are guides to the eye to indicate the strongest final states up to 10 eV energy transfer. The features around 35 eV energy transfer are tentatively assigned to ligand orbitals that hybridize with W 4f orbitals.

gives access to dipole forbidden transitions and can hence probe the density of states with various angular momentum numbers [16]. For example, rare-earth compounds have their lowest-energy excited states too high in angular momentum to be accessible by any spectroscopy obeying the dipole selection rule. This has recently been shown for the N$_{4,5}$ edges of La and Ce compounds, where at large q strong multiplet lines characteristic of the 4f final states were observed [17]. Due to powerful X-ray sources and improved analyzer instrumentation the number of applications of XRS has dramatically increased over the last years. Current instruments are specialized on either measuring a whole range of q values simultaneously (see e.g. [18]), or getting a high efficiency (large solid angle) over a smaller q range, in either the low q (dipole) or high q (non-dipole) limit. Several such instruments are employed at synchrotron facilities, including SPring8, APS, ESRF, and SSRL.

Non-resonant XES

X-ray emission is a second-order process: First, a core hole is created and the X-rays that are emitted when this core hole is filled give rise to the X-ray emission or fluorescence (cf. Figure 1). The chemical sensitivity in XES can be due to two mechanisms [19]. If the core hole is replaced by another core hole, e.g. a 3p to 1s (Kβ) transition in a 3d transition metal, the sensitivity to the valence electrons is indirect. The final state core hole interacts with the valence electrons and this interaction shapes the emission line. The Kβ lines, for example, are sensitive to the valence shell spin state. This has been exploited to study water oxidation in photosynthesis [20] or in high pressure applications in

earth science [21]. The Kβ lines can also be used to record spin-selective absorption spectra providing a unique tool to study the 3d shell configuration [22].

XES can also probe the valence shell directly. In this case, the energy of the emission spectrometer is tuned close to the Fermi level. It has been shown that these emission lines are very sensitive to the ligand orbitals of 3d transition metals and thus the type of ligand can be identified [23]. At the L-edges of 5d transition metals it is possible to probe the metal d-electrons directly. Such experiments are comparable to valence shell photoemission with different selection rules. However, XES is bulk sensitive, strictly element-selective, and has the advantage that no high vacuum is required while the energy resolution is usually higher in photoemission experiments. Extending the XES energy range to lower energies to reach, for example, S and Cl brings opportunities for studies in desulphurization catalysis as well as methane activation and chlorine removal studies.

Resonant XES (RXES) and resonant inelastic X-ray scattering (RIXS)

The spectral shape of fluorescence lines depends on the way the core hole is created. Tuning the incident energy to an absorption edge one can observe the spectral changes in XES as a function of the incident energy. There are two major advantages in this approach. First, the absorbing atom is not ionized in case of resonant excitations as the photoexcited electron stays within a bound state. Second, the spectral features become sharper because the lifetime of the final state now determines the broadening (this is, in fact, the reason for the sharpening

effect in HERFD XAS). RXES allows one to measure L-edge like spectra using hard X-rays in 3d transition metals [24]. The sensitivity is high enough to record spectra even on dilute samples such as metal-loproteins [25].

It is useful in resonant spectroscopies to define the difference between incident and emitted energy as the energy transfer (cf. Figure 1). When reducing this energy transfer to a few eV one finds new spectral features, some of which have been identified with ligand to metal charge transfer and local dd excitations [26]. The energy transfer scale in resonant inelastic X-ray scattering (RIXS) is equivalent to optical spectroscopy but is not limited to 6.2 eV as in standard UV-Vis spectroscopy. The selection rules in RIXS are different from UV-Vis because of the two-photon process and optically forbidden transitions become accessible. The spectra require a careful theoretical analysis because of polarization and momentum transfer dependencies. The potential of this technique in the chemical sciences is considerable because valence shell excitations are observed by means of an element selective, hard X-ray technique.

Outlook

Instrumentation for photon-out analysis at synchrotron radiation sources has made enormous progress. While research on magnetic materials has been pushing for high energy resolution ($\triangle E < 100$ meV), it is more important for applications in chemistry to capture a large solid angle at moderate energy resolutions of a few hundreds of meV up to a few eV. Catalysis research with low metal concentrations and its need for *in-situ* studies is one of the major research fields to benefit from these developments. Photon-out spectroscopy on catalysts with less than 1 wt% metal concentration is now feasible and the limit is decreasing with improving instrumentation. The existing in-situ cells for fluorescence detected XAS can be readily installed on an X-ray spectrometer. Several designs for X-ray spectrometers exist that could be implemented on XAS beamlines.

It will furthermore become more and more important to have user-friendly theoretical codes that can model these new spectroscopies. The excellent developments in the analysis and calculation of EXAFS serve as a good example and it is desirable that a similar quality and ease of use will be achieved for XES. Finally, photon-in photon-out X-ray spectroscopy has the potential to play a major role in future single-shot and pump-probe experiments at X-ray free electron lasers. Here, energy-dispersive analyzer setups will make it possible to instantly record the spectrum of the scattered photons.
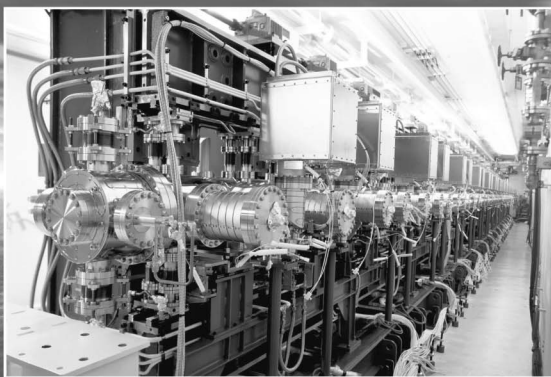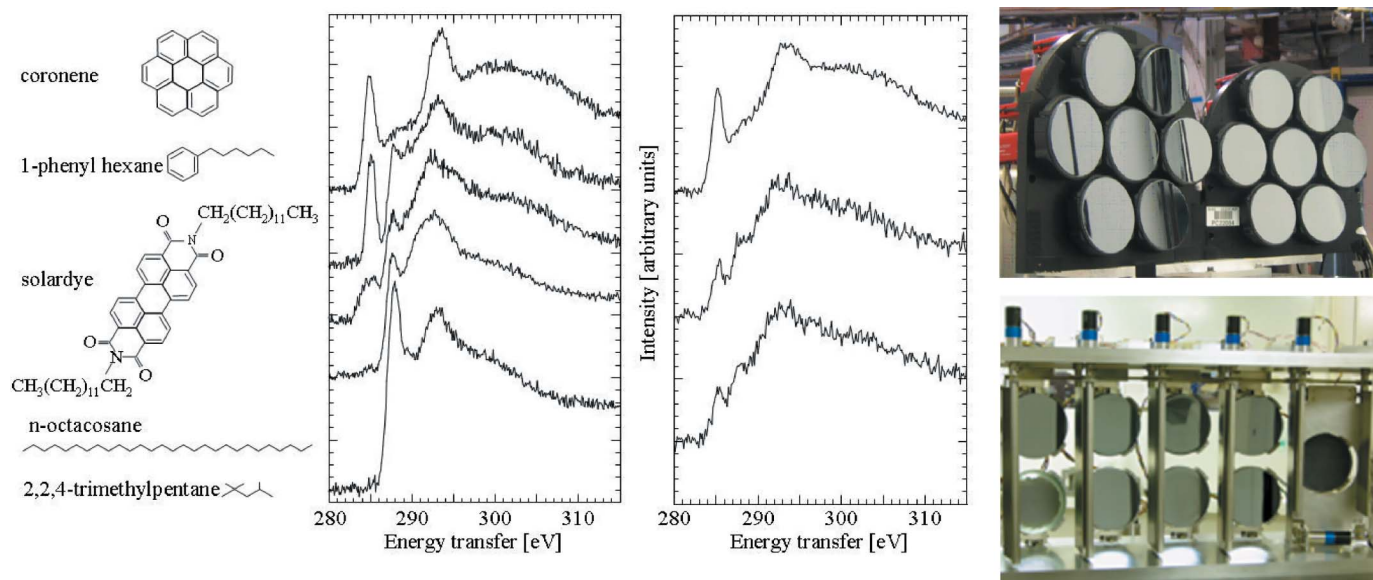
Figure 3: Left: Comparison of hydrocarbon XRS spectra with varying degrees of aromatic to saturated carbon. Spectra correspond to compounds shown left (top to bottom: coronene, 1-phenyl hexane, solardye, n-octacosane, 2,2,4-trimethylpentane). Center: Asphaltene spectra, top: Tanito Harum coal, middle: Venezuela #20 crude, bottom: KUHM crude. Combinations of hydrocarbon spectra are used to characterize composition of asphaltenes (see [13], first reference). Right: XRS instruments at SSRL (top) and ESRF (bottom) showing the Si analyzer crystals that are either clustered or spread depending on what kind of measurement with respect to the momentum transfer q is desired.

References

1. We include in the term "scattering" also fluorescence as it can be treated within the same formalism as RIXS, i.e. the Kramers-Heisenberg equation.
2. P. Glatzel and U. Bergmann, *Coord. Chem. Rev*. **249**, 65 (2005).
3. W. Schülke, *Electron Dynamics by Inelastic X-Ray Scattering* (Oxford University Press, Oxford, 2007); J. Hoszowska, et al., *Nucl. Instr. and Meth. A* **376**, 129 (1996); K. Sakurai and H. Eba, *Jpn. J. Appl. Phys. Part 1* **38**, 650 (1999); U. Bergmann and S. P. Cramer, in *Crystal and Multilayer Optics* (SPIE, San Diego, 1998), Vol. 3448, p. 198; H. Hayashi, et al., *J. Electron Spec. Rel. Phen*. **136**, 191 (2004); E. Welter, et al., *J. Synch. Rad*. **12**, 448 (2005); S. Huotari, et al., *Rev. Sci. Instrum*. **77** (2006); A. C. Hudson, et al., *Rev. Sci. Instrum*. **78** (2007); J. P. Hill, et al., *J. Synch. Rad*. **14**, 361 (2007); B. Dickinson, et al., *Rev. Sci. Instrum*. **79**, 123112 (2009).
4. F. M. F. de Groot and A. Kotani, *Core Level Spectroscopy of Solids* (Taylor and Francis, New York, 2008).
5. A similar, i.e. wavelength dispersive, approach to solve the non-linearity problem of solid state detectors is followed when using Laue analyzers or multilayers.
6. P. Glatzel, et al., *Phys. Rev. B* **72,** 014117 (2005).
7. J. Yano, et al., *J. Am. Chem. Soc*. **127**, 14974 (2005).
8. K. Hämäläinen, et al., *Phys. Rev. Lett*. **67**, 2850 (1991); H. Hayashi, *Anal. Sci*. **24**, 15 (2008).
9. D. Radu, et al., *J. Phys. Chem. C* **112**, 12409 (2008); W. M. Heijboer, et al., *Cat. Tod*. **110**, 228 (2005).
10. P. Carra, et al., *Phys. Rev. Lett*. **74**, 3700 (1995).
11. P. W. Loeffen, et al., *Phys. Rev. B* **54**, 14877 (1996).
12. O. V. Safonova, et al., *J. Phys. Chem. B* **110**, 16162 (2006); J. A. van Bokhoven, et al., *Ang. Chem*. **45**, 4651 (2006).
13. U. Bergmann and O. C. Mullins, in *Asphaltene, Heavy Oils and Petroleomics*, edited by O. C. Mullins, E. Y. Sheu, A. Hammami and A. G. Marshall (Springer, New York, 2006), p. 139; U. Bergmann, et al., *Chem. Phys. Lett*. **369**, 184 (2003); U. Bergmann, et al., *Petrol. Sci. Technol*. **22**, 863 (2004).
14. P. Wernet, et al., *Science* **304**, 995 (2004); U. Bergmann, et al., *Phys. Rev. B* **76**, 024202 (2007); U. Bergmann, et al., *J. Chem. Phys*. **127**, 174504 (2007).
15. P. Wernet, et al., *J. Chem. Phys*. **123**, 15403 (2005); Y. Q. Cai, et al., *Phys. Rev. Lett*. **94**, 025502 (2005); W. L. Mao, et al., *Science* **314**, 636 (2006); S. K. Lee, et al., *P. Natl. Acad. Sci. USA* **105**, 7925 (2008); Y. Meng, et al., *P. Natl. Acad. Sci. USA* **105**, 11640 (2008); J. S. Tse, et al., *Phys. Rev. Lett*. **100,** 095502 (2008).
16. M. H. Krisch, et al., *Phys. Rev. Lett*. **78**, 2843 (1997); H. Sternemann, et al., *Phys. Rev. B* **75**, 075118 (2007); T. T. Fister, et al., *J. Am. Chem. Soc*. **130**, 925 (2008).
17. R. A. Gordon, et al., *EPL* **81**, 26004 (2008).
18. T. T. Fister, et al., *Rev. Sci. Instrum*. **77**, 063901 (2006).
19. A. Meisel, et al., *X-Ray Spectra and Chemical Binding* (Springer-Verlag, New York, 1989).
20. J. Messinger, et al., *J. Am. Chem. Soc*. **123**, 7804 (2001).
21. J. Badro, et al., *Science* **300**, 789 (2003).
22. K. Hämäläinen, et al., *Phys. Rev. B* **46**, 14274 (1992); G. D. Pirngruber, et al., *J. Phys. Chem. B* **110**, 18104 (2006); P. Glatzel, et al., *Phys. Rev. B* **77**, 115133 (2008).
23. U. Bergmann, et al., *Chem. Phys. Lett*. **302**, 119 (1999); V. A. Safonov, et al., *J. Phys. Chem. B* **110**, 23192 (2006).
24. F. M. F. de Groot, et al., *J. Phys. Chem. B* **109**, 20751 (2005).
25. P. Glatzel, et al., *J. Am. Chem. Soc*. **126**, 9946 (2005).
26. C. C. Kao, et al., *Phys. Rev. B* **54**, 16361 (1996); S. Huotari, et al., *Phys. Rev. B* **78**, 041102 (2008).